Evaluating adipocyte differentiation of bone marrow-derived mesenchymal stem cells by a deep learning method for automatic lipid droplet counting

Leila Hassanlou[a], Saeed Meshgini[a,*], Effat Alizadeh[b,c]

[a] Department of Biomedical Engineering, Faculty of Electrical and Computer Engineering, University of Tabriz, Tabriz, Iran
[b] Drug Applied Research Center, Faculty of Advanced Medical Sciences, Tabriz University of Medical Sciences, Tabriz, Iran
[c] Department of Medical Biotechnology, Faculty of Advanced Medical Sciences, Tabriz University of Medical Sciences, Tabriz, Iran

A B S T R A C T

Stem cells are a group of competent cells capable of self-renewal and differentiating into osteogenic, chondrogenic, and adipogenic lineages. These cells provide the possibility of successfully treating patients. During differentiation into adipose tissues, a large number of lipid droplets normally accumulate in these cells, which can be seen through oil red O staining. Although the oil red O staining technique is regularly used for assessing the differentiation degree, its validity for quantitative studies has not been approved yet. Lipid droplet counting has applications in differentiation works and saves time and costs once being automated. In this research, for proving the differentiation of mesenchymal stem cells (MSCs) into adipocyte tissues, their microscopic images were provided. Then, the microscopic images were segmented into square patches, and the lipid droplets were annotated through single-point annotation. The proposed network, based on deep learning, is a fully convolutional regression network processing an image with a small respective field on it. Finally, this method not only does count the lipid droplets but also generates a count map. The average counting accuracy is 94%, which is higher than that of the state-of-the-art methods. It is useful to cell biologists to check the percentage of differentiation in different samples. Also, with a count map, it is possible to observe the regions with high concentrations of lipid droplets without oil red O staining and, thus, examine the total adipocyte differentiation. The contribution of this paper is that a deep learning algorithm has been used for the first time in the field of processing intracellular images.

1. Introduction

The research on stem cells was triggered by the findings of two Canadian scientists named Ernest McCulloch and James Till in the 1960s [1]. A stem cell is a potent cell, and this potency is the basis for the attention directed to these cells. Moreover, the interests and challenges in the field of stem cells arise from the fact that these cells provide the patients suffering from diseases and disabilities with the feasibility of living. Among these cells, the mesenchymal stem cells are substantially important due to their ease of access and proliferation. Their potency characterizes these cells for differentiation into osteogenic, chondrogenic, and adipogenic lineages [2]. The presence of these cells in the bone marrow was reported for the first time by Friedenstein et al. [3]. Later on, Owen et al. [4] demonstrated the potency of these cells *in vivo* by transplanting mesenchymal stem cells into rabbits.

Adipose tissue engineering is a growing field focused on the current clinical needs for the adipose tissue pathologies. Soft tissue replacement is necessary when a disease damages the adipose tissues of different body organs. Soft tissue deficiencies may be caused by several factors, including traumas, tumor resection, congenital anomalies, and infections. The clinical solution to soft tissue deficiencies involves natural and synthetic materials and implants. Since each of these factors may result in damage, it seems necessary to develop new treatments based on stem cells. The adipose tissue is the key to soft tissue reconstruction.

When the mesenchymal stem cells are placed in an adipocyte differentiation medium, lipid droplets accumulate in them. Over time, these lipid droplets are formed, cover the entire cell diameter, and expand.

Cell counting is a current challenge to biological research. Specialists use various cell markers to count the cells manually. However, due to the lack of high contrast, the disarrangement of a large number of cells, obstruction, the need for adjustment of microscope

* Corresponding author. Room No. 207, Faculty of Electrical and Computer Engineering, University of Tabriz, 29 Bahman Blvd, Tabriz, Iran, Postal Code: 5166616471.
E-mail addresses: leila.hassanlou94@ms.tabrizu.ac.ir (L. Hassanlou), meshgini@tabrizu.ac.ir (S. Meshgini), alizadehe@tbzmed.ac.ir (E. Alizadeh).

parameters, the diversity of cell sizes, and the morphological properties, it is difficult to count the cells manually. Moreover, this process entails constant care and concentration and is highly time-consuming and exhausting. The results are also descriptive and can considerably vary by subjective interpretation. Consequently, manual counting has been replaced by automated counting due to the increasing demand for cell analysis. Because, given the image data obtained, manual counting is inefficient and even impossible. Automated cell counting determines the number of certain cells in a microscopic image, which is of interest in a wide range of medical scenarios [4–6].

According to the computer vision community, automated cell counting is a sub-discipline of object counting. Cell counting is addressed from two standpoints.

1 Detection-based counting, which involves detection and classification. This approach is often used for a certain cell type [7–9].
2 Regression-based counting, which disregards detection and obtains the number of cells directly from the images [10,11].

Previous studies suggested that the latter approach is quicker and more accurate than detection-based methods.

Recently, deep learning has been widely used in the field of computer vision, and convolutional neural networks have become popular in the analysis of microscopic images. Counting methods based on deep learning have proliferated recently [8]. In the study conducted by Villa et al. [9], to count cells with several frames, the ConvNets and LSTM (long short-term memory) neural networks were utilized. In the study by Hernández et al. [10], cell counting was carried out by combining a pyramid network and a VGG neural network to propose an approach based on the convolutional neural networks. Xue et al. [11] described a supervised training framework with several convolutional neural networks, and the cells were counted through a regression problem by annotating all cells for supervised training. Chen et al. [12] used a deep learning regression network to count the mitoses based on the histological images prepared for the diagnosis of cancer. Xie et al. [13] proposed two fully convolutional regression networks for automated cell counting to count the cells and provide a density map of the entire image.

In cell biology, counting particles in intracellular images is vital to study the causes of diseases, though it is carried out manually by operators, which is highly time-consuming and produces subjective outcomes. Moreover, the design and development of automated counting give a deeper insight into counting. However, the computer-assisted counting of particles in intracellular images is a new research project and has not become conventional yet. Recently, with the advancements in microscopic research and cytology staining, it has been possible to see the intracellular structures. These images are called intracellular images, enabling cell biologists to count the number of intracellular particles and ascertain relationships between pathologic factors [14,15].

Since intracellular image processing is a newly emerging technology, a common intracellular image processing technique has not been developed yet. Hence, there is no conventional automated counting method for intracellular images and, in return, operators must practice manual counting. Manual counting exposes the operators to intense physical and mental stress, preventing them from processing multiple images. Moreover, intracellular images are created with high magnification, and their subsequent lack of clarity causes the error.

Although the study on intracellular image processing has begun, optimal algorithms and techniques are fewer than other medical image processing techniques. However, intracellular image processing has been addressed in some recent papers. These papers proposed particle tracking, detection, and counting. As regards tracking, researchers have employed dynamic programming [16], and Bayesian [17] approaches.

In the detection of adipocytic phenotype, different methods have been used, including intracellular accumulation of lipid droplets and
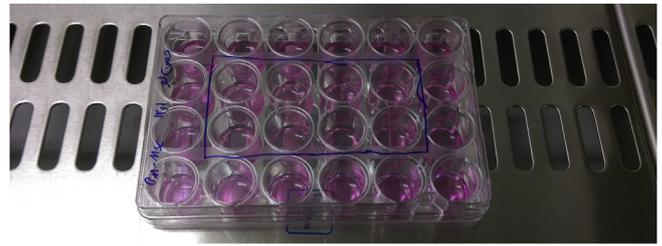

Fig. 1. The plate contained adipocyte differentiation medium and mesenchymal stem cells. The cells were incubated for 21 days in the differentiation medium, and the medium was changed every three days.

evaluation of transcription of adipocyte lineage genes [18]. Another reported method for evaluation is the detection of adiponectin in the medium. A report showed that the data of adiponectin secretion are strongly associated with oil red O method of quantification at the final step of adipogenesis [19]. Although using real-time PCR or western blotting for proving transcription or protein upregulation of adipocyte phenotype is a gold standard, they are expensive and need more time. Hence, oil red O staining is possibly the shortest way for evaluation of adipogenesis. Still, it is a time-consuming method, necessitating more work and materials, and preparation for new dye. Also, as a limitation, oil red O dye cannot label different polar lipids, including phospholipids, ceramides, and sphingolipids [20].

Using automatic counting techniques can be an alternative to routine experimental methods mentioned above to prevent possible errors and save time and costs.

However, very few studies have been conducted on intracellular lipid droplet counting. In the study by Sims et al. [21], image processing techniques such as thresholding were used to count lipid droplets without staining.

In 2012, Kumguy et al. [22] used a support vector machine (SVM) approach [23] to count lipid droplets and estimate the radius of each droplet in fluorescent images that were visible under the light. However, machine learning techniques have been rarely used in intracellular image processing. Later on, in 2015, a method was proposed in another study [24] for the automated counting and estimation of particle radii based on pattern recognition techniques. In this method, particles were analyzed by a computer through two processes. In phase one, particles were detected by dint of a support vector machine and face recognition. Next, the points on the edge of each particle were detected and differentiated by virtue of the intensity difference between the particle and the background. The points on edge were extracted through voting and a circle. The proposed technique offered higher accuracy compared to ImageJ [25].

In 2016, Kumguy et al. [26] proposed a counting method based on regression analysis. They used the mask patterns for higher-order local autocorrelation (HLAC) [27], partial least squares regression [28], and the autocorrelation between two different types of features. The proposed method was more accurate than the principal component regression, support vector regression, and ImageJ techniques. In the previous three papers, the fluorescent images of lipid droplets were used. In addition to these methods, Cellprofiler [29] and MetaMorph [30] analysis software solutions have been used to count the lipid droplets.

The present study aims at using a deep learning algorithm for the first time in the field of processing intracellular images and counting lipid droplets along with generating a count map to examine total adipocyte differentiation. It is an effective method for studying adipocyte differentiation in the assessment of cell population density.
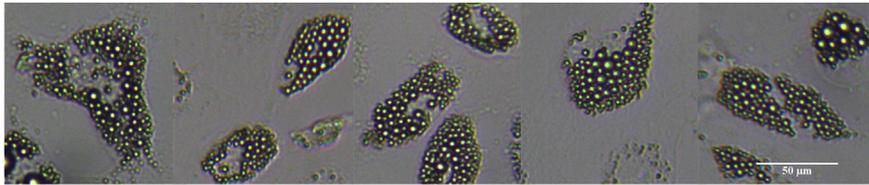
Fig. 2. Microscopic images of lipid droplets resulting from the differentiation of mesenchymal stem cells into adipose tissue. These microscopic images were obtained by a × 40 inverted optical microscope without oil red O staining. Lipid droplets have a complicated structure and are highly dense in some regions. They are also found in different sizes. (For interpretation of the references to color in this figure legend, the reader is referred to the Web version of this article.)

2. Materials and methods

2.1. Culture and differentiation

Mesenchymal stem cells were isolated from the Femur bone marrow of mice. To obtain a cell line, the isolated cells were cultured consecutively to reach passages number 3 to 5. Afterward, the surface markers were analyzed through flow cytometry (FACS). The cells were placed in an adipocyte differentiation medium, and the lipid droplets appeared after 21 days. It is necessary to count and study the density of lipid droplets and cell morphologies to calculate the total differentiated cells (%). Conventionally, lipid droplets are studied through oil red O staining [31], which helps count and see the stained lipid droplets. Stained cells can be analyzed using a microscope, and stains heighten the contrast of lipid droplets [21]. One of the limitations to the use of staining is that other lipids not associated with the intracellular lipid droplets also change color. Furthermore, this method requires cell fixation, which may result in deformations and transfer of lipid droplets, hampering the analysis. Moreover, manually counting lipid droplets can be difficult. High costs of these methods and the differences in the interpretations of experts are other drawbacks of manual counting. Hence, lipid droplets were studied without oil red O staining in this research. Fig. 1 shows an image of a plate containing the adipocyte differentiation medium and mesenchymal cells.

2.2. Imaging

Images were obtained by an inverted Hund Wetzlar optical microscope, a digital CCD camera, and an imaging software program (× 40) with a resolution of 1200 × 1600. Fig. 2 shows several microscopic images obtained. To inhibit size variations of the original microscopic image (i.e. to avoid loss of information) and to increase the training data (i.e. to prevent overfitting), they were divided into 300 × 300 images, and a dataset consisting of 200 images was finally prepared. For all images, the image annotation tool with image masks[1] was used to create ground truth as a single-pixel annotation.

The annotation was the labeling as a single-pixel almost on the center of each lipid droplet because labeling with dots was much easier than drawing the boundaries for lipid droplets. This work was completed under the supervision of a stem cell differentiation specialist to ensure that the annotation was done correctly. Afterward, the data based on the evaluation protocol used by Lempitsky and Zisserman [7] were classified into three categories, namely training data, validating data, and testing data. This protocol has been used by papers such as Xie et al. [13] and Cohen et al. [32].

3. Theory

3.1. Redundant counting with regression convolutional network

Deep learning is emerging as a powerful tool that has brought considerable success to the analysis of microscopic images. CNN is one of the most significant deep learning techniques. This network consists of convolutional and pooling layers, which function similar to the human visual system [33].

Generally, image data are the input to a CNN, which form an input layer and yield a vector of the distinctive features of object classes as the output layer. Hidden layers form a series of convolutions and pooling layers between the input and output layers [34]. Network training is done through several forward and backward propagation steps based on the predicted output and the annotated ground truth. In the backpropagation phase, the gradient of each parameter is calculated based on loss costs. All parameters are updated based on gradients to calculate the next forward propagation. Network training can also be stopped following the adequate number of iterations.

In this research, deep learning and convolutional neural networks (CNNs) were used for the automated lipid droplet counting in differentiated stem cells. The redundant counting approach proposed by Cohen et al. [32] was also applied. In this method, an image was processed in a fully convolutional network to obtain a matrix revealing the lipid droplets count in a 32 × 32 respective field. The receptive field in the convolutional network is part of the input space that affects a specific unit of the network. Generally, the term "receptive field" is used when the final network output is linked to the network input (the network input image).

By processing an image in the fully convolutional network method [35], each image pixel was calculated several times during image processing. The number of windows containing a given pixel equals the window size (i.e., 32 × 32 = 1024). To obtain the real number, all of these predictions were averaged. For the counting process, the quantity of each lipid droplet was calculated several times deliberately to obtain the average probable errors. In the redundant counting, if the pixel annotation is not located precisely at the center of the lipid droplet or is outside of it, the network can still be trained because the lipid droplet is manifested in the receptive field on average.

The regression network also predicted the number of lipid droplets in the receptive field. As a result, the overfitting was firstly diminished since the fully convolutional network parameters decreased at a small network size. Secondly, by segmenting the image, CNN received more training data to set the parameters.

3.1.1. Input
Our goal was to count the target objects in image I. This image contained multiple target objects annotated through single-point annotation. Since the network reduced dimensions only from (32 × 32) to (1 × 1), the input boundary must be expanded to confront the objects that were manifested in it, because the objects on the image boundary were generally in the receptive field overlapping with only one column or row in the input image.

3.1.2. Target image
The target image shows the desired output for a given input. The target image can be extracted from a map, L, by annotating a point equal in size to the input image I, where every object is annotated with a unit pixel. Moreover, let $R(x,y)$ be a set of pixel positions in the receptive field of $T(x,y)$. Therefore, the target image, T, can be obtained as follows.

$$T(x, y) = \sum_{(x',y') \in R(x,y)} L(x', y')$$

(1)

Fig. 3. Proposed network architecture. There are inception units in the middle layers of the network. These units contain 3 × 3 (pad = 1) and 1 × 1 (pad = 0) convolutional layers, which do not alter the tensor size.

Table 1
Detailed information for each layer of the proposed network.

Layer type	Kernel Size	Number of Kernels	Padding	Output
Convolutional	3 × 3	64	32	362 × 362 × 64
Inception	1 × 1 conv	16	0	362 × 362 × 32
	3 × 3 conv	16	1	
Inception	1 × 1 conv	16	0	362 × 362 × 48
	3 × 3 conv	32	1	
Convolutional	14 × 14	16	0	349 × 349 × 16
Inception	1 × 1 conv	136	0	349 × 349 × 168
	3 × 3 conv	32	1	
Inception	1 × 1 conv	64	0	349 × 349 × 128
	3 × 3 conv	64	1	
Inception	1 × 1 conv	64	0	349 × 349 × 96
	3 × 3 conv	32	1	
Inception	1 × 1 conv	40	0	349 × 349 × 136
	3 × 3 conv	96	1	
Convolutional	18 × 18	32	0	332 × 332 × 32
Convolutional	1 × 1	64	0	332 × 332 × 64
Convolutional	1 × 1	64	0	332 × 332 × 64
Convolutional	1 × 1	1	0	332 × 332 × 1

Where *T(x,y)* is the set of lipid droplets in an *r × r* receptive field. As a result, it becomes the regression target for the *r × r* region of the image. A 32 × 32 square kernel equal in size to the receptive field was used for creating the target image to train the network.

3.1.3. Combining counts

Due to counting each lipid droplet multiple times, with a stride of 1, each target was counted once for each pixel in its receptive field. So, the redundant counts can be defined as follows.

$$\text{Redundant counts} = \left(\frac{r}{s}\right)^2 \tag{2}$$

Where *r* is the dimension of the receptive field and s stands for stride. In order to recover the real count, the sum of all pixels was divided by the number of redundant counts and the real count is defined as follows.

$$\text{Real count} = \frac{\sum_{x, y} F(I)[x, \ y]}{\text{Redundant counts}} \tag{3}$$

Where *F(I)* is the map of predicted counts for *I*.

3.1.4. Network structure

The network proposed by Cohen belonged to the inception networks family because the inception units were placed at the center of the network so that 1 × 1 and 3 × 3 convolutions functioned without any tensor size variation. After each convolution, leaky ReLUs and batch normalization were performed, followed by the removal of the pooling layer. As compared to the convolutional network proposed by Cohen, the results were enhanced by changing the number of inception units and their kernels. Fig. 3 depicts the proposed network structure. The 332 × 332 count map was generated as the output of a 300 × 300 image. Also, Table 1 presents details of each layer of the network.

3.2. Training

The Adam optimization method [36] was used to train a network at a learning rate of 0.00002 and with a batch size of 2, offering high computational capacity and low memory usage as some of its advantages. Moreover, *L*1 was selected as the error function, which is the sum of the absolute total difference between real and predicted values. This loss was a replacement objective to the real count.

Firstly, an initial *MAE* error was assumed for validation data. Then training was done for 1000 epochs. In each epoch for the network, specific weights were set, and validation data error was calculated. If the value of the validation data error.

In each epoch was less than the initial error value and also lower

Original Image

True Count=101   Predict Count=105

True Count=178   Predict Count=173

True Count=100   Predict Count=103

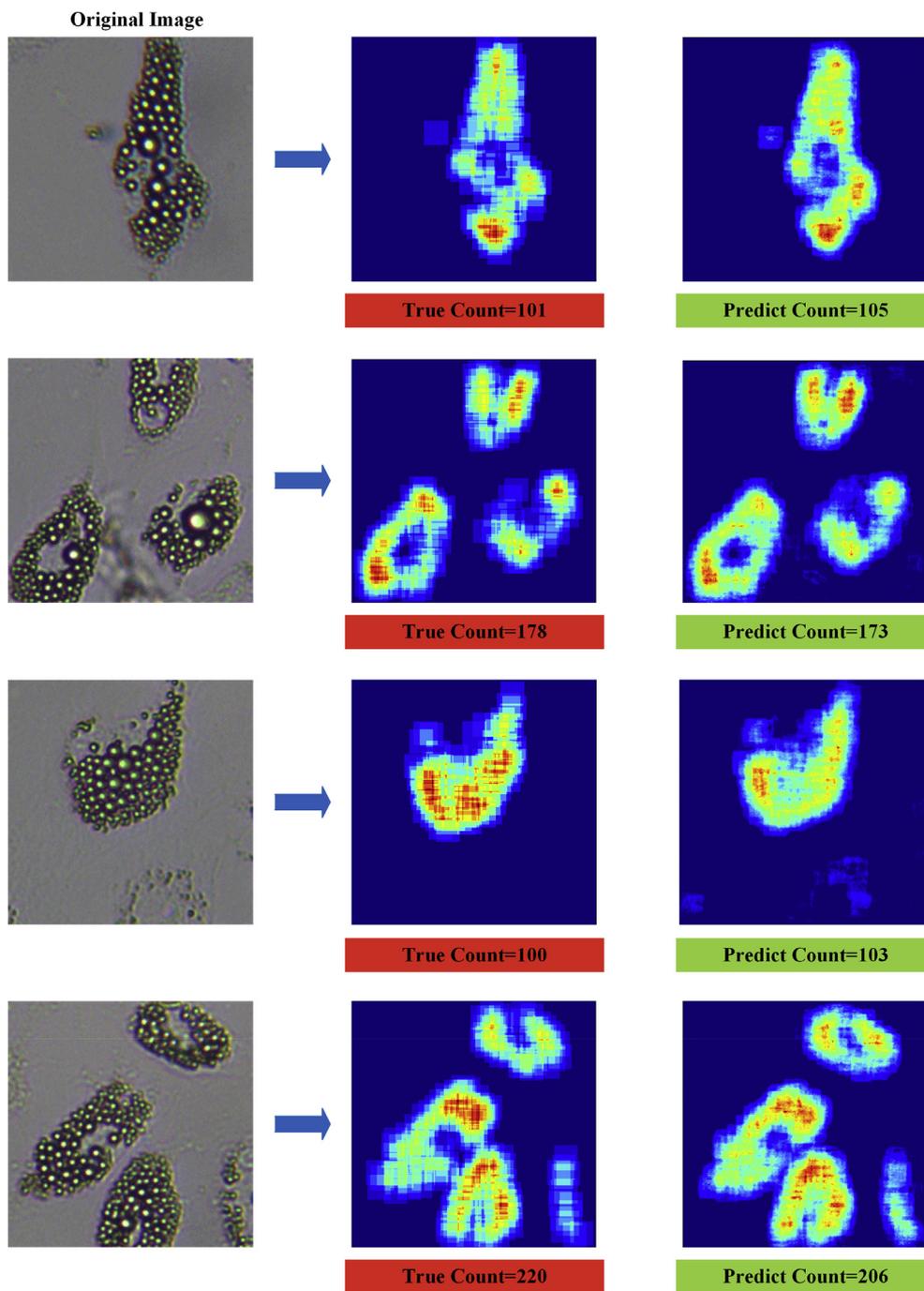True Count=220   Predict Count=206

Fig. 4. The counting results and count map of 4 different images of the test data. The left image shows the original cells, and the middle and right images present the count map, the total ground truth count, and the predicted output.

than the error threshold that we set its value at 11, it was updated as the lowest validation error, and then the error of the test data was calculated. So the best network model was saved. This process was repeated until the end of the training, and the network with the proper weights and the least error was ultimately obtained. It is worth stating that the network weights were assigned to use Xavier method [37] adjusted for ReLU gain. In this paper, N represents the number of training data.

4. Results

A network was developed using Theano [38], which is a Python library designed to contribute to the definition, optimization, and assessment of mathematical expression. It was implemented on Valohai, a

deep learning management platform, using a Tesla V100-SXM2-16GB/ 64 GB GPU. 32 and 64 data items were used for the first and second rounds of training, respectively, and the same amount of validation data was considered. Finally, the network was evaluated with 100 test data items.

Fig. 4 presents the comparison of four test images using the true and predicted count results. As can be seen, the predicted number of lipid droplets is acceptably close to the real number of lipid droplets. On the other hand, the cells differentiated into adipose tissues are easily recognizable on the count map, and there is no need for oil red O staining and its possible dangers. As seen, none of the image impurities has been considered as a lipid droplet. The dominant color in those parts of the image, where the lipid droplets are more concentrated and tinier, is
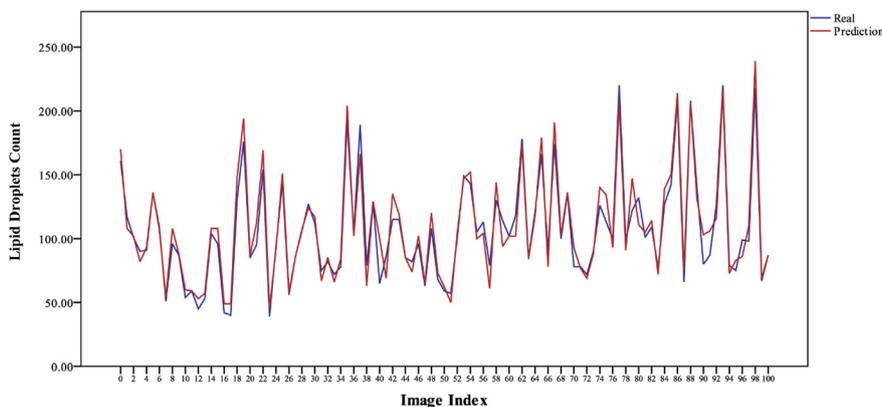
Fig. 5. Comparison of the true and predicted counts using the test data (N = 32). Evidently, the count predicted using some of the data is close to the true count, but there are considerable differences between the results obtained using the other data.
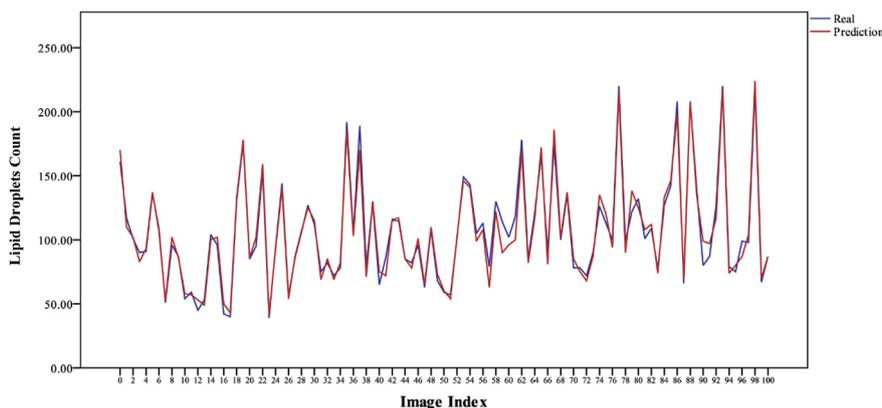

Fig. 6. Comparison of the true and predicted counts using the test data (N = 64). As compared to N = 32, the predicted count is extremely close to the true count for most data, and thus, the training for N = 64 yields acceptable results.

Table 2
Mean *Accuracy* with 100 images.

Method	Average Accuracy (%)
ImageJ	75.6
Cohen's Method (N = 32)	89.91
Cohen's Method (N = 64)	92.57
Proposed Method (N = 32)	91.45
Proposed Method (N = 64)	**94.45**

Table 3
Mean *MAE* with 100 images.

Method	MAE
ImageJ	27
Cohen's Method (N = 32)	9.742574
Cohen's Method (N = 64)	7.346535
Proposed Method (N = 32)	8.415842
Proposed Method (N = 64)	**5.386139**

warmer and closer to red, reflecting the essence of the count map. As seen in the original photo, some of the lipid droplets are so tiny that it is challenging to recognize and count them.

Besides, due to the high magnification of the images, they have low resolution. These results are useful for analyzing the overall differentiation (%) of mesenchymal stem cells into adipose tissues and the recognition of the differentiated cells without oil red O staining in different samples.

In all experiments, we used the *MAE* (Mean Absolute Error) as the metric for the quantitative assessments. *K* shows the total number of test images, and t_i and p_i denote the real and predicted values, respectively.

MAE is defined as follows.

$$MAE = \frac{1}{K} \sum_{i=1}^{K} |t_i - p_i| \tag{4}$$

Accuracy is also defined as follows.

$$Accuracy(\%) = \left[1 - \frac{|t_i - p_i|}{|t_i|} \right] \times 100 \tag{5}$$

Figs. 5 and 6 present the comparison between the true and predicted counts using 100 test data items. Evidently, better results were obtained when the network was trained by 64 data items.

In general, one of the advantages of the proposed method is that it trains the network with a fewer number of data items because networks are trained in deep learning problems with a very large data set.

5. Discussion

A comparison was made between the counts using ImageJ and Cohen's approach. ImageJ is a software program used to process and analyze images via its plugins. This software and image processing techniques, such as thresholding, were used to count the lipid droplets. Table 2 presents the mean accuracy obtained using 100 test data items, the aforementioned methods, and the proposed method. The *MAEs* of the values are also listed in Table 3.

As can be seen, ImageJ had low accuracy and a high error rate because of high magnification and low resolution of intracellular
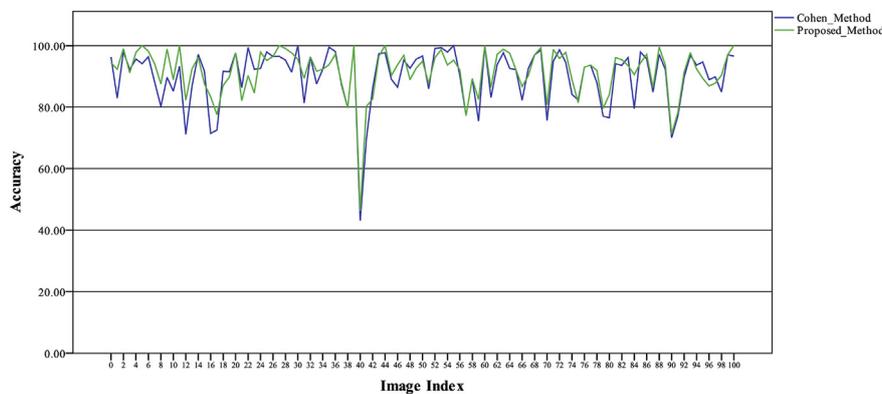
Fig. 7. Comparison of counting accuracy based on Cohen's network and the proposed network (N = 32). Accuracy varies between 45% and 100%, and the accuracy of the proposed method is higher than Cohen's method for most data.
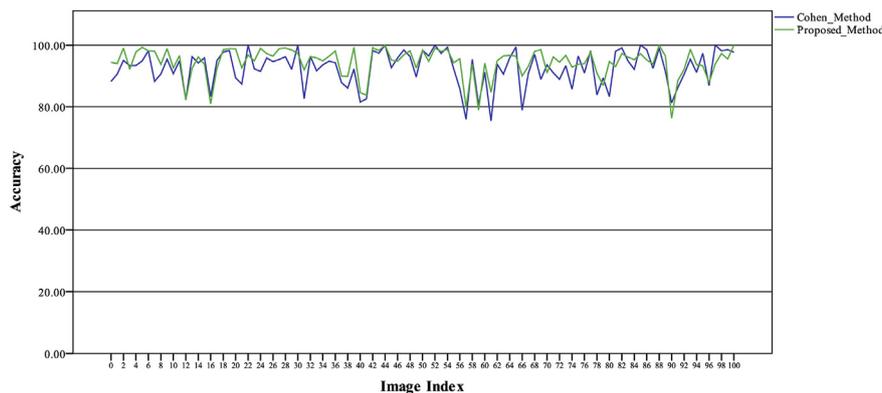

Fig. 8. Comparison of counting accuracy based on Cohen's network and the proposed network (N = 64). Accuracy varies between 78% and 100%, showing a considerable increase compared to the accuracy obtained for N = 64. Moreover, the accuracy of the proposed method is higher than Cohen's method for most data.

images. The method based on the network proposed by Cohen also offered low accuracy and higher error rates. Fig. 7 illustrates the comparison between the counts resulted from Cohen's method and our proposed method using 100 test data items (for $N = 32$). Fig. 8 also presents the results for $N = 64$. As can be observed, the accuracy varied between 45% and 100% for $N = 32$. Furthermore, in most data items, the accuracy of the proposed method was higher than Cohen's method. Moreover, for $N = 64$, the accuracy ranged from 78% to 100%, showing considerable growth compared to $N = 32$. Here, the accuracy of the proposed method was found to be higher than Cohen's method for most data.

6. Conclusions

According to the results presented in this paper, it is extremely easier and more accurate to count the lipid droplets in the mesenchymal stem cells differentiated into adipose tissues using a method based on a convolutional regression network, compared to the oil red O staining method and manual counting, entailing cell fixation and resulting in exhaustion and different interpretations. Other advantages of this method include time and cost savings. It is also possible to compare the total adipocyte differentiation (%) in different samples by producing a count map.

After preparing the count map, it has been feasible to calculate the total adipocyte differentiation (%) in different samples. In this paper, deep learning was used for the first time to process intracellular images. By training the proposed convolutional regression network using two training datasets on Valohai, the outcome was assessed based on 100 images. The quantitative results indicated the acceptable performance of this method compared to the reference method. It was also found out

that the accuracy of the proposed network was more acceptable than the other methods. The constraints on this research included multiple contaminations of the mesenchymal stem cells and the iteration of the 21-day differentiation process. The limitation on the proposed method was also its inability to obtain the exact position of the lipid droplets. However, the number of lipid droplets is more important than their positions for obtaining the percentage of differentiation of stem cells into adipose tissues.

Besides, it could be stated that cell biologists can calculate the total number of differentiated cells by calculating the average number of lipid droplets. In this respect, the number of lipid droplets is counted in some selected cells in the image, and the average number is calculated. Afterward, using the total number of lipid droplets calculated through the proposed technique, the number of differentiated cells is obtained.

Appendix A. Supplementary data

Supplementary data to this article can be found online at https://doi.org/10.1016/j.compbiomed.2019.103365.

References

[1] Y. Wan, Bone marrow mesenchymal stem cells: fat on and blast off by FGF21, Int. J. Biochem. Cell Biol. 45 (3) (2013) 546–549.

[2] M.C. Ciuffreda, G. Malpasso, P. Musarò, V. Turco, M. Gnecchi, Protocols for in vitro differentiation of human mesenchymal stem cells into osteogenic, chondrogenic and adipogenic lineages, in: M. Gnecchi (Ed.), Mesenchymal Stem Cells: Methods And Protocols, Springer New York, New York, NY, 2016, pp. 149–158.

[3] A.J. Friedenstein, K. V Petrakova, A.I. Kurolesova, G.P. Frolova, Heterotopic of Bone Marrow. Analysis of Precursor Cells for Osteogenic and Hematopoietic Tissues, *Transplantation*, 1968.

[4] P. Bianco, P.G. Robey, P.J. Simmons, Mesenchymal stem cells: revisiting history, concepts, and assays, Cell Stem Cell 2 (4) (2008) 313–319.

[5] A. Coates, A. Ng, Selecting receptive fields in deep networks, NIPS (News Physiol. Sci.) (i) (2011) 1–9.

[6] C. Arteta, V. Lempitsky, J.A. Noble, A. Zisserman, "Interactive Object Counting," *Lect.* Notes Comput. Sci. (Including Subser. Lect. Notes Artif. Intell. Lect. Notes Bioinformatics) vol. 8691, LNCS, 2014, pp. 504–518 PART 3.

[7] V. Lempitsky, A. Zisserman, Learning to count objects in images, Adv. Neural Inf. Process. Syst. (2010) 1324–1332.

[8] M. Rahnemoonfar, C. Sheppard, Deep count: fruit counting based on deep simulated learning, Sensors 17 (4) (2017) 1–12.

[9] A.G. Villa, A. Salazar, I. Stefanini, Counting Cells in Time-Lapse Microscopy Using Deep Neural Networks, (2018).

[10] C.X. Hernández, M.M. Sultan, V.S. Pande, Using Deep Learning for Segmentation and Counting within Microscopy Data, (2018).

[11] Y. Xue, N. Ray, J. Hugh, G. Bigras, Cell Counting by Regression Using Convolutional Neural Network vol. 9913, (2016), pp. 274–290.

[12] H. Chen, X. Wang, P.A. Heng, Automated mitosis detection with deep regression networks, 2016-June, Proc. - Int. Symp. Biomed. Imaging (2016) 1204–1207.

[13] W. Xie, J.A. Noble, A. Zisserman, Microscopy cell counting and detection with fully convolutional regression networks, Comput. Methods Biomech. Biomed. Eng. 6 (3) (2018) 283–292.

[14] S. Sakaushi, K. Senda-Murata, S. Oka, K. Sugimoto, Visualization of aberrant peri-nuclear microtubule aster organization by microtubule-destabilizing agents, Biosci. Biotechnol. Biochem. 73 (5) (2009) 1192–1196.

[15] S. Sakaushi, et al., Dynamic behavior of FCHO1 revealed by live-cell imaging microscopy: its possible involvement in clathrin-coated vesicle formation, Biosci. Biotechnol. Biochem. 71 (7) (2007) 1764–1768.

[16] K. Fujisaki, et al., Detection and tracking protein molecules in fluorescence microscopic video, Proceedings - 2013 1st International Symposium On Computing And Networking, vol. 2013, CANDAR, 2013, pp. 270–274.

[17] T. Okabe, K. Hotta, "Accuracy Improvement of Melanosome Tracking by Error Correction," in *2013 International Conference On Digital Image Computing: Techniques And Applications*, DICTA), 2013, pp. 1–8.

[18] T. Fink, V. Zachar, Adipogenic differentiation of human mesenchymal stem cells, Methods Mol. Biol. 698 (2011) 243–251.

[19] E. Martella, C. Bellotti, B. Dozza, S. Perrone, D. Donati, E. Lucarelli, Secreted adiponectin as a marker to evaluate in vitro the adipogenic differentiation of human mesenchymal stromal cells, Cytotherapy 16 (11) (2014) 1476–1485.

[20] M.C.V.P. Fabricio da Mota Ramalho Costa, Sabrina Alves, Chyntia Díaz and 1Oswaldo Cruz Foundation (Brazil), "Procedures for the Staining of Lipid Droplets with Oil Red O,", (2018).

[21] J.K. Sims, B. Rohr, E. Miller, K. Lee, Automated image processing for spatially resolved analysis of lipid droplets in cultured 3t3-L1 adipocytes, Tissue Eng. C Methods 21 (6) (2015) 605–613.

[22] S. Kumagai, K. Hotta, Counting and radius estimation of lipid droplet in intracellular images, Conf. proc. - IEEE int. conf. syst. man cybern. 2012, pp. 67–71.

[23] V.N. Vapnik, Statistical learning theory, Interpreting 2 (1998) 736.

[24] S. Kumagai, K. Hotta, Particle detection in intracellular images and radius estimation by circle fitting, IEEJ Trans. Electr. Electron. Eng. 10 (2) (2015) 181–185.

[25] M. D. Abràmoff, I. Hospitals, P. J. Magalhães, and M. Abràmoff, "Image Processing with ImageJ.".

[26] S. Kumagai, K. Hotta, Particles counting in intracellular images by partial least squares regression and HLAC feature between multiple features, Electron. Commun. Jpn. Part I Commun. 99 (8) (2016) 3–12.

[27] N. Otsu, T. Kurita, A new scheme for practical, flexible and intelligent vision systems, IAPR Work. Comput. Vis. (1988) 431–435.

[28] H. Wold, Soft modelling by latent variables: the non-linear iterative partial least squares (NIPALS) approach, J. Appl. Probab. 12 (S1) (1975) 117–142.

[29] V. Campos, B. Rappaz, F. Kuttler, G. Turcatti, O. Naveiras, High-throughput, non-perturbing quantification of lipid droplets with digital holographic microscopy, J. Lipid Res. 59 (7) (Jul. 2018) 1301–1310.

[30] M. Dragunow, R. Cameron, P. Narayan, S. O'Carroll, Image-based high-throughput quantification of cellular fat accumulation, J. Biomol. Screen 12 (7) (2007) 999–1005.

[31] K.S. Arezoumand, et al., The emu oil emulsified in egg lecithin and butylated hydroxytoluene enhanced the proliferation, stemness gene expression, and in vitro wound healing of adipose-derived stem cells, In Vitro Cell. Dev. Biol. Anim. 54 (3) (2018) 205–216.

[32] J.P. Cohen, G. Boucher, C.A. Glastonbury, H.Z. Lo, Y. Bengio, Count-ception: counting by fully convolutional redundant counting, 2018-Janua, Proc. - 2017 IEEE Int. Conf. Comput. Vis. Work. ICCVW 2017, 2018, pp. 18–26.

[33] S. Filipe, L.A. Alexandre, RETRACTED ARTICLE: from the human visual system to the computational models of visual attention: a survey, Artif. Intell. Rev. 43 (4) (2015) 601.

[34] T. Liu, S. Fang, Y. Zhao, P. Wang, J. Zhang, Implementation of training convolutional neural networks, Computer Vision and Pattern Recognition (2015) abs/1506.0, arXiv:1506.01195v2 [cs.CV].

[35] J. Long, et al., Fully convolutional networks for semantic segmentation, Proc IEEE Comput. Soc. Conf. Comput. Vis. Pattern Recognit. (2015) 1–9 07-12-June, no. i.

[36] D. Kingma, J. Ba, Adam: a Method for Stochastic Optimization, (2014), pp. 1–13 *arXiv Prepr. arXiv1412.6980*.

[37] X. Glorot, Y. Bengio, Understanding the difficulty of training deep feedforward neural networks, PMLR 9 (2010) 249–256.

[38] R. Al-Rfou, et al., Theano: A Python framework for fast computation of mathematical expressions, Symbolic Computation (2016) abs/1605.0, arXiv:1605.02688v1 [cs.SC].

Leila Hassanlou received the B.E. (2014) in electrical and electronics engineering from University of Urmia, Urmia, Iran, and the M.S. (2018) in biomedical engineering from University of Tabriz, Tabriz, Iran. Her current research interests include pattern recognition, machine learning, deep learning, and their applications in medical image processing.

Saeed Meshgini received the Ph.D. (2013) in electrical engineering from University of Tabriz, Tabriz, Iran. He is currently an assistant professor in the Faculty of Electrical and Computer Engineering at University of Tabriz, Tabriz, Iran. His research interests include digital signal processing, processing of biomedical signals and images, soft computing and machine learning, pattern recognition and biometrics.

Effat Alizadeh received the Ph.D. (2015) in medical biotechnology from Tabriz University of Medical Sciences, Tabriz, Iran. She is currently an assistant professor in the Faculty of Advanced Medical Sciences at Tabriz University of Medical Sciences, Tabriz, Iran. Her research interests include stem cell biology and differentiation, RNA interference biology and technology, tissue engineering and cell therapy, epigenetics, and microRNAs.